Journal of Water Process Engineering

One-Step Synthesized 3D-Structured MOF Foam for Efficient and Convenient Catalytic Reduction of Nitrogen-containing Aromatic Compounds

--Manuscript Draft--

Manuscript Number:	JWPE-D-20-02774R1
Article Type:	Full Length Article
Keywords:	HKUST-1; Cu foam; 4-Nitrophenol; Reduction; methylene blue
Corresponding Author:	Kun-Yi Lin National Chung Hsing University Taichung, TAIWAN
First Author:	Jia-Yin Lin
Order of Authors:	Jia-Yin Lin
	Pen-Yuan Chen
	Eilhann Kwon
	Wen Da Oh
	Siming You
	Chao-Wei Huang
	Farshid Ghanbari
	Thomas Wi-Afedzi
	Kun-Yi Lin
Abstract:	Metal Organic Frameworks (MOFs) receive increasing attention for 4-nitrophenol (4-NP) reduction; however the existing studies of using MOFs for 4-NP reduction all involve with noble metals. Moreover, the reported MOFs are very fine powders which are inconvenient for realistic implementation. Thus, the present study proposes to develop a MOF foam which exhibits macroscale features of foam and microscale functionalities of MOFs. Specifically, a Cu foam is selected as the macroporous substrate which serves as a porous support and the metal source for synthesizing Cu-based MOF, HKUST-1, via an one-step electrochemical method. The resulting HKUST-1 foam can act as a convenient catalyst for reduction of 4-NP to 4-AP in either batch-type or flow-thru-type reactions. The corresponding E_a of 4-NP reduction (43.3 kJ/mol) is also significantly lower than E_a values of reported catalysts, including noble metal catalysts, whereas the corresponding TOF (48.3 min^{-1}) is higher than many other catalysts. HKUST-1 foam can also efficiently catalyze reduction of methylene blue (MB) to fully decolorize its color. In addition, HKUST-1 foam could be reused over multi-cycles and retain its activity for reduction of 4-NP and MB. These features validate that HKUST-1 foam is a practical, convenient, and reusable catalyst for reduction of 4-NP.
Suggested Reviewers:	Hongqi Sun Edith Cowan University h.sun@ecu.edu.au Advanced Oxidation Processes; wastewater treatments
	Shaobin Wang University of Adelaide shaobin.wang@adelaide.edu.au environmental catalysis, nanocatalysts
	Sambandam Anandan National Institute of Technology sanand@nitt.edu environmental catalysis, nanocatalysts
	Mojtaba Amini

One-Step Synthesized 3D-Structured MOF Foam for Efficient and Convenient Catalytic Reduction of Nitrogen-containing Aromatic Compounds

Jia-Yin Lin[a], Pen-Yuan Chen[b], Eilhann Kwon[c], Wen Da Oh[d], Siming You[e], Chao-Wei Huang[f], Farshid Ghanbari[g,], Thomas Wi-Afedzi[a] and Kun-Yi Andrew Lin[a,*]*

[a]Department of Environmental Engineering & Innovation and Development Center of Sustainable Agriculture & Research Center of Sustainable Energy and Nanotechnology, National Chung Hsing University, 250 Kuo-Kuang Road, Taichung, Taiwan

[b]Department of Landscape Architecture, National Chiayi University, Chiayi, Taiwan

[c]Department of Environment and Energy, Sejong University, 209 Neungdong-ro, Gunja-dong, Gwangjin-gu, Seoul, Republic of Korea

[d]School of Chemical Sciences, Universiti Sains Malaysia, 11800 Penang, Malaysia

[e]James Watt School of Engineering, University of Glasgow, Glasgow G12 8QQ, UK

[f]Department of Chemical and Materials Engineering, National Kaohsiung University of Science and Technology, Kaohsiung, Taiwan

[g]Department of Environmental Health Engineering, Abadan Faculty of Medical Sciences, Abadan, Iran

*Corresponding Authors. E-mail addresses: linky@nchu.edu.tw (KYA Lin); ghanbari.env@gmail.com (F. Ghanbari).

Abstract

Metal Organic Frameworks (MOFs) receive increasing attention for 4-nitrophenol (4-NP) reduction; however the existing studies of using MOFs for 4-NP reduction all involve with noble metals. Moreover, the reported MOFs are very fine powders which are inconvenient for realistic implementation. Thus, the present study proposes to develop a MOF foam which exhibits macroscale features of foam and microscale functionalities of MOFs. Specifically, a Cu foam is selected as the macroporous substrate which serves as a porous support and the metal source for synthesizing Cu-based MOF, HKUST-1, via an one-step electrochemical method. The resulting HKUST-1 foam can act as a convenient catalyst for reduction of 4-NP to 4-AP in either batch-type or flow-thru-type reactions. The corresponding activation energy (E_a) of 4-NP reduction (43.3 kJ/mol) is also significantly lower than E_a values of reported catalysts, including noble metal catalysts, whereas the corresponding TOF (48.3 min^{-1}) is higher than many other catalysts. HKUST-1 foam can also efficiently catalyze reduction of methylene blue (MB) to fully decolorize its color. In addition, HKUST-1 foam could be reused over multi-cycles and retain its activity for reduction of 4-NP and MB. These features validate that HKUST-1 foam is a practical, convenient, and reusable catalyst for reduction of 4-NP.

Keywords: HKUST-1, Cu foam, MOFs, 4-Nitrophenol, Reduction, methylene blue

1.Introduction

Nitro or nitrogen-containing aromatic compounds represent essential pollutants in industrial effluents [1]. Among these N-containing aromatic species, 4-nitrophenol (4-NP) particularly receives great attention as 4-NP can cause damages to human's central nervous and blood systems [2, 3]. Therefore, many approaches have been proposed to eliminate 4-NP from water, such as biological degradation [4], adsorption [5], chemical oxidation, photocatalytic degradation [6] and catalytic reduction [7]. Out of these approaches, catalytic reduction of 4-NP appears as the most promising one because the nitro-group of 4-NP can be converted to an amine group, resulting in 4-aminophenol (4-AP), which is much less toxic and even valuable for synthesizing other fine chemicals [8-10].

To reduce 4-NP to 4-AP catalytically, transition metals and reducing agents are usually necessitated [3,6,7]. Specifically, many noble metals, including Au, Pd, Ru, and Pt, have been adopted for reducing 4-NP to 4-AP by using $NaBH_4$ as a reducing agent [8–12]. Nevertheless, high expenses of noble metals pose huge challenges for large-scale implementation of this technique. Therefore, it is greatly-desired to develop non-noble-metal catalysts for 4-NP reduction.

Recently, a novel class of coordination materials, Metal Organic Frameworks (MOFs), is developed and applied extensively because MOFs, comprised of metals and organic ligands, can exhibit various porous/hierarchical structures, with miscellaneous functions [13]. Metal sites of MOFs have been also proven to catalyze various reactions [11-14] and thus MOFs should be a promising alternative for catalyzing 4-NP reduction [15, 16]. While several MOFs have been discussed and studied for reduction of 4-NP [17-21], these reported MOFs were comprised of noble metals (e.g., Ag) or functionalized with noble metal particles (e.g., Ag, Au, Pd). Very few studies have

certainly looked into investigating catalytic activities of non-noble-metal MOFs themselves. Besides, these reported MOFs are usually very fine powders, making them less practical and inconvenient for realistic implementation. Thus, it would be crucial to explore the catalytic activities of non-noble metal MOFs without usage of any noble metals. Moreover, it would be also critical to immobilize MOFs on substrates, which can be macroscale and porous for convenient use and maximization of the loading of MOFs and exposure of MOFs to reactants.

More critically, such as MOF-immobilized macroscale substrate should be easily prepared without complicated procedures and long preparation time to make such a MOF-composite more realistic. To this end, the present study proposes to employ a metal foam, copper foam specifically, as the substrate which not only serves as a macroscale and hierarchically porous support for MOFs but also acts the metal source for synthesizing MOFs. The copper (Cu) foam is particularly selected as Cu has been validated as a non-noble metal for reducing 4-NP and moreover Cu can be adopted to synthesize the most classical MOF, HKUST-1. Via one-step electrochemical method, in which the organic ligand of 1,3,5-benzenetricarboxylic acid (H_3BTC) would react with Cu^{2+} of Cu foam to grow a layer of HKUST-1 on the surface of foam. This feature is very distinct from conventional physical attachment of MOFs on foam-like substrates which require complicated multiple steps [22], and have problems of instability [23] and disorder growth and aggregation of MOFs on foam-like substrates [24-26]. Therefore, such a HKUST-1 foam has many promising advantages of convenient macroscale features of foam and microscale functionalities of HKUST-1, and it should be a very useful and practical catalyst for 4-NP reduction. Unfortunately, HKUST-1 foam has never been investigated for its catalytic activity in aqueous catalytic reductive applications, and thus the present study would provide valuable information for

fabricating such a composite, and important findings and scientific insights into catalytic characteristics of HKUST-1 foam.

2. Experimental

2.1 Materials

All regents in the study were analytical-regent grade and used without further purification. Cu foam was provided by May Chun Company Limited, Taiwan. Copper nitrate ($Cu(NO_3)_2$) was obtained from Union Chemicals (Taiwan). 1,3,5-benzenetricarboxylic acid (H_3BTC) was purchased from Showa Chemical Co. Ltd (Taiwan). Sodium Borohydride ($NaBH_4$) was obtained from Sigma-Aldrich (USA).

2.2 Preparation of HKUST-1 foam catalyst

The preparation of HKUST-1 foam via the electrochemical synthesis can be illustrated in Fig. 1. First, Cu foam(1×1.5 cm) with a thickness of 1 mm, and 95 pores per inch (PPI) was washed with 3M HCl solution for 15 min then rinsed with distilled water and ethanol for several times. Subsequently, Cu foam and carbon rod were used as anode and cathode, respectively, in an electrochemical reactor. The distance between two electrodes was kept as 2.5 cm, and 0.1g H_3BTC was directly added into 100 ml of ethanol/water mixture (1:1) to afford the electrolyte solution. The anodizing growth of HKUST-1 on the Cu foam was implemented at 5V for 30 min at room temperature as displayed in Fig. 1(b). Next, the resultant HKUST-1 foam was washed by distilled water thoroughly and dried at 65^{o}C in oven overnight to afford HKUST-1 foam.

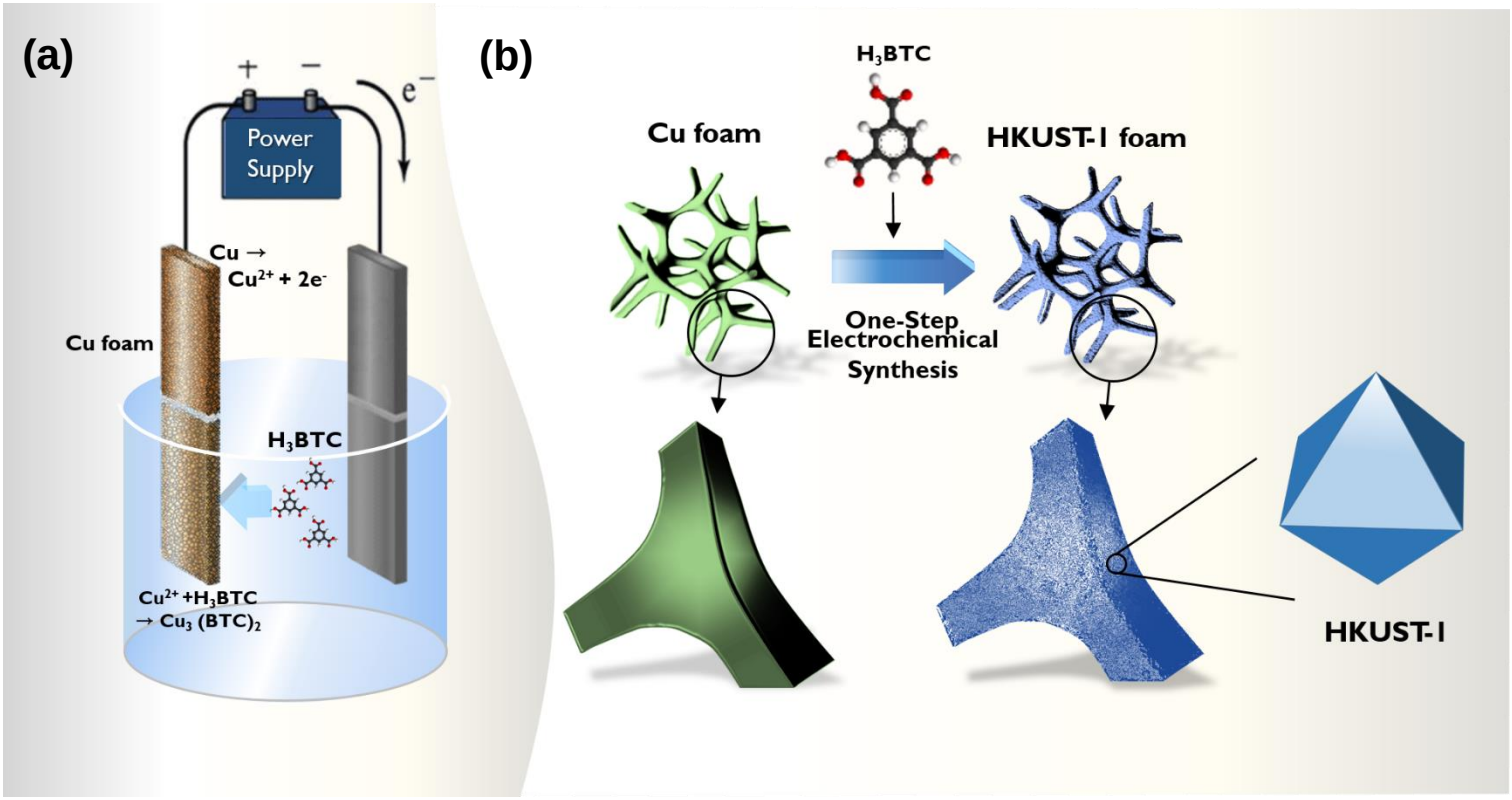

Fig. 1. Schematic illustration for preparation of HKUST-1 foam via the one-step electrochemical synthesis.

2.3 Characterization of HKUST-1 foam

The morphologies of HKUST-1 foam were determined by FE-SEM (JEOL JSM-7800F, Japan). The XRD pattern of HKUST-1 foam was measured with an X-ray diffractometer (Bruker D8 Discover, USA). X-ray photoelectron spectroscopy (XPS) was also adopted to analyze surface chemistry of HKUST-1 foam (PHI 5000, ULVAC-PHI, Japan). Textural properties of HKUST-1 foam were determined using a volumetric gas adsorption analyzer (ANTON PAAR NOVATOUCH LX2, Austria) for obtaining

N_2 adsorption/desorption isotherms.

2.4 Catalytic reduction of 4-nitrophenol and Methylene Blue

In a typical experiment of 4-NP reduction, an aqueous solution of 4-NP was first prepared at the concentration of 3.6×10^{-3} M, and $NaBH_4$ was prepared at the concentration of 4.2 M. In a 100 ml beaker containing 47.5 ml distilled water, 2.5 ml of 3.6×10^{-3} M 4-NP solution was introduced and 0.2 ml $NaBH_4$ of 4.2 M was added at a desired temperature, a piece of HKUST-1 foam (3.5 mg) was added subsequently. The reaction of 4-NP reduction to 4-AP was implemented in a large excess $NaBH_4$ to ensure negligible influence of the donor BH_4^- on reaction kinetics in order to assume that the reaction rate can therefore be independent on the concentration of $NaBH_4$ [27, 28]. After pre-set intervals, UV-vis spectra of reactants were recorded over the scanning region of 200-500 nm. The quantitative determination of 4-NP was performed by recording the absorbance at different time intervals at 400 nm. Catalytic reduction of MB experiments followed similar step as in 4-NP reduction. However, UV-vis spectra of MB were recorded over the scanning region of 450-750 nm with its quantitative determination after different intervals at 664 nm.

3. Results and discussion

3.1 Characterization of Cu foam and HKUST-1 foam

Fig. 2(a) shows photographs of pristine Cu foam and HKUST-1 foam. The pristine Cu foam exhibited the typical reddish brown color of Cu. After the anodic synthesis with H_3BTC, the Cu foam's color changed from reddish brown to blue, which is the typical color of HKUST-1. The variation of color suggested that the surface of the foam had been deposited with HKUST-1, and the fraction of HKUST-1 accounted for *ca*. 7 wt%

of the entire HKUST-1 foam based on gravimetric measurements.

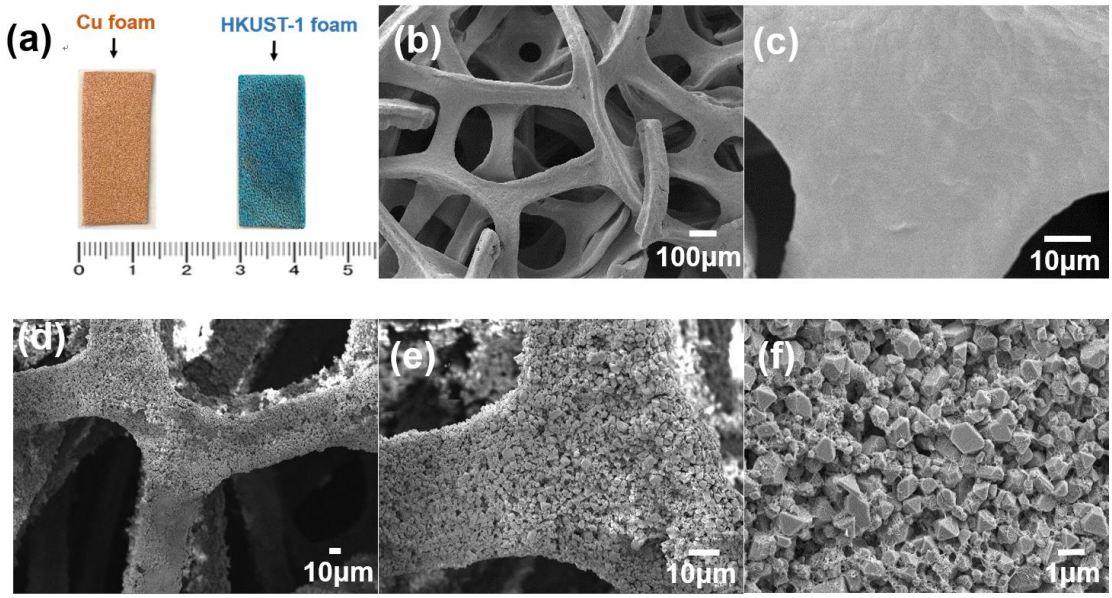

Fig. 2. (a) Photographs of Cu foam and HKUST-1 foam, (b-c) SEM images of the pristine Cu foam, (d-f) SEM images of HKUST-1 foam under different magnifications,

To further realize the variation on the surface of foam, the surficial morphologies of Cu foam and HKUST-1 foam were examined by SEM. Fig. 2 (b-c) shows the SEM image of pristine Cu foam, which exhibited the typical micro-structures of foam with smooth surfaces. On the other hand, the SEM image of HKUST-1 foam (Fig. 2(d)) still maintained the micro-structure of foam but its surface had been deposited with a layer of fine particles. The closer view (Fig. 2 (e-f)) reveals that these fine particles exhibited polyhedral morphologies (e.g., octahedrons) with sizes of 0.5 ~ 3 μm, which were similar to the reported sizes of HKUST-1 [29-31]. The corresponding elemental mapping results also suggested that Cu and O were homogenous distributed over Cu foam (Fig. S1). To further verify species of these polyhedral particles, the crystalline structures of the pristine and modified foam were determined in Fig. 3(a). As the pristine Cu foam exhibited very typically few peaks at 43.2 and 50.4°, corresponding to (111) and (200) planes of Cu, respectively [32, 33], the modified foam showed a

series of additional peaks in the range of 8 - 50°, and these peaks can be well-indexed to the simulated XRD pattern of HKUST-1 [30, 34, 35], confirming that the layer of polyhedral fine particles deposited on the foam was HKUST-1, and the modified foam was validated as HKUST-1 foam.

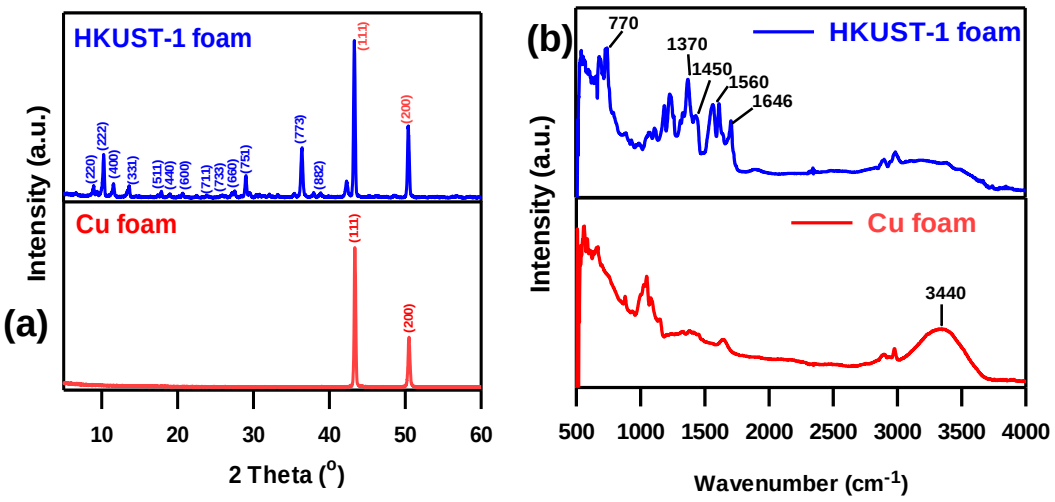

Fig. 3. (a) XRD patterns (b)FTIR spectra of Cu foam and HKUST-1 foam.

Moreover, IR spectra of HKUST-1 foam and the pristine Cu foam were also measured to realize chemical variation of foam before and after the electrochemical modification in Fig. 3(b). In the case of pristine Cu foam, the broad peak located at 3440 cm^{-1} corresponded to the stretching vibration absorption of –OH groups at Cu foam surfaces [32]. After the growth of HKUST-1 on the Cu foam, the resulting HKUST-1 foam exhibited a series of significant peaks in the range of 1000~2000 cm^{-1}. The band in the range of 500-1600 cm^{-1} region can be attributed to HKUST-1 consisting of H_3BTC and –OH group at >3000 cm^{-1} [36]. Hence, the band at 770 cm^{-1} was attributed to Cu-O stretching vibration [37] and the band at 1370cm^{-1} was assigned to the symmetric vibrations center [36]. The bands at 1450-1560cm^{-1} were attributed to carboxylic group of H_3BTC [38]. The band at 1646 cm^{-1} resulted from aromatic C=C and 1718cm^{-1} from COO^- of H_3BTC [18, 35, 39]. These peaks further confirmed the

successful formation of HKUST-1 on the Cu foam.

Moreover, as HKUST-1 foam was a composite consisting micro-scale HKUST-1 and the macro-scale foam, its textural properties would be interesting and then investigated. Fig. 4(a) shows the N_2 sorption isotherms of the pristine Cu foam and HKUST-1 foam. N_2 sorption isotherm is employed to determine surface areas and pore volumes of porous materials by measuring amounts of N_2 adsorbed onto porous media [40]. The higher volume adsorbed indicates that the tested substrate exhibits a larger surface area and pore volume, whereas the lower volume adsorbed suggests a lower surface area and pore volume. While the N_2 sorption amount of Cu foam was very low, leading to a low surface area of 20 m^2/g, HKUST-1 foam exhibited a tremendously higher N_2 sorption and thus showed a substantially higher surface area of 209 m^2/g owing to the growth of HKUST-1 on the Cu foam. The pore volume of HKUST-1 was 0.184 cm^3/g (Fig. 4(b)), which was also significantly higher than that of the pristine Cu foam as 0.017 cm^3/g, showing that the textural properties of Cu foam was considerably enhanced because of growth of HKUST-1.

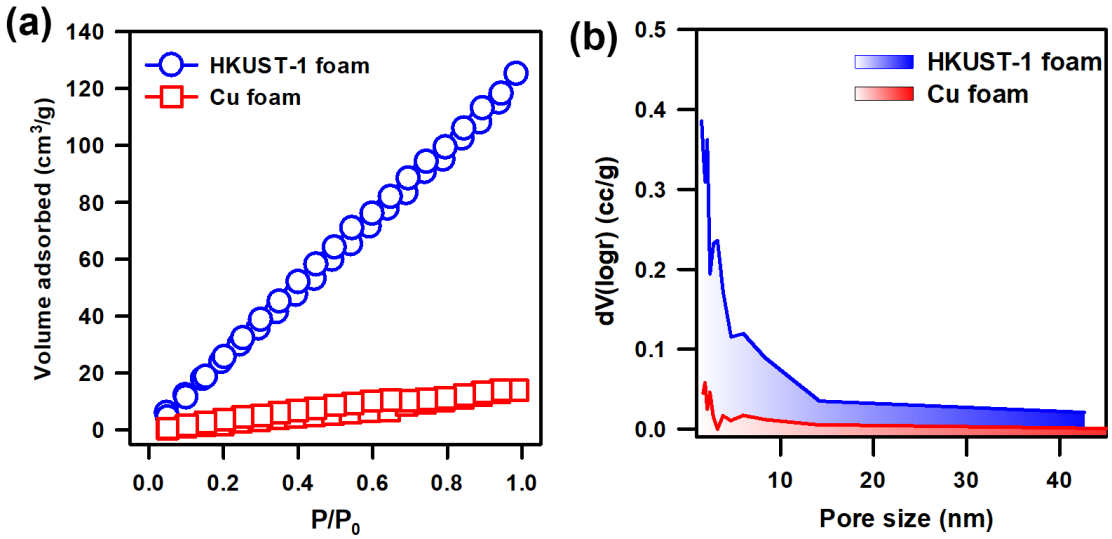

Fig. 4. (a) N_2 sorption isotherms and (b) pore size distributions of the pristine Cu foam and HKUST-1 foam.

3.2 Catalytic reduction of 4-nitrophenol by HKUST-1 foam

Prior to examining catalytic activities of HKUST-1 foam for 4-NP reduction, it was necessary to verify whether 4-NP would be removed simply via adsorption to HKUST-1. Fig. 5(a) shows that UV-Vis spectrum of 4-NP in the presence of HKUST-1 foam was very close to that of the pristine 4-NP solution, indicating that HKUST-1 foam itself could not eliminate or reduce 4-NP even after 300 min. However, the peak area and height of 4-NP slightly decreased in the presence of HKUST-1 foam, indicating that a small fraction of 4-NP was absorbed into HKUST-1foam. When the reducing agent, $NaBH_4$, was introduced to 4-NP solution, the color of 4-NP solution changed from light yellow to bright yellow due to the deprotonation of 4-NP [41], and correspondingly, the maximum peak shifted from 316 nm to 400 nm. Subsequently, a piece of HKUST-1 foam was added, the peak of 4-NP at 400 nm decreased rapidly and almost vanished within 15 min as shown in Fig. 5(b). Meanwhile, one can notice that the peak of 4-AP grew notably, demonstrating that the conversion of 4-NP to 4-AP was accomplished within a short time and no by-product was observed in view of the isosbestic point.

In addition to the batch-type demonstration of using HKUST-1 foam to reduce 4-NP to 4-AP, HKUST-1 foam could be also employed as a membrane catalyst for flow-thru-type reactions. Fig. 5(c) shows a syringe containing a yellowish solution of 4-NP. Once the syringe was pushed to pass the yellowish 4-NP solution through HKUST-1 foam, the yellowish solution readily became transparent. The filtrate was also analyzed and only 4-AP was detected without any 4-NP remained (Fig. 5(e)). This successfully revealed that HKSUT-1 foam is an effective, versatile and convenient catalyst for 4-NP reduction.

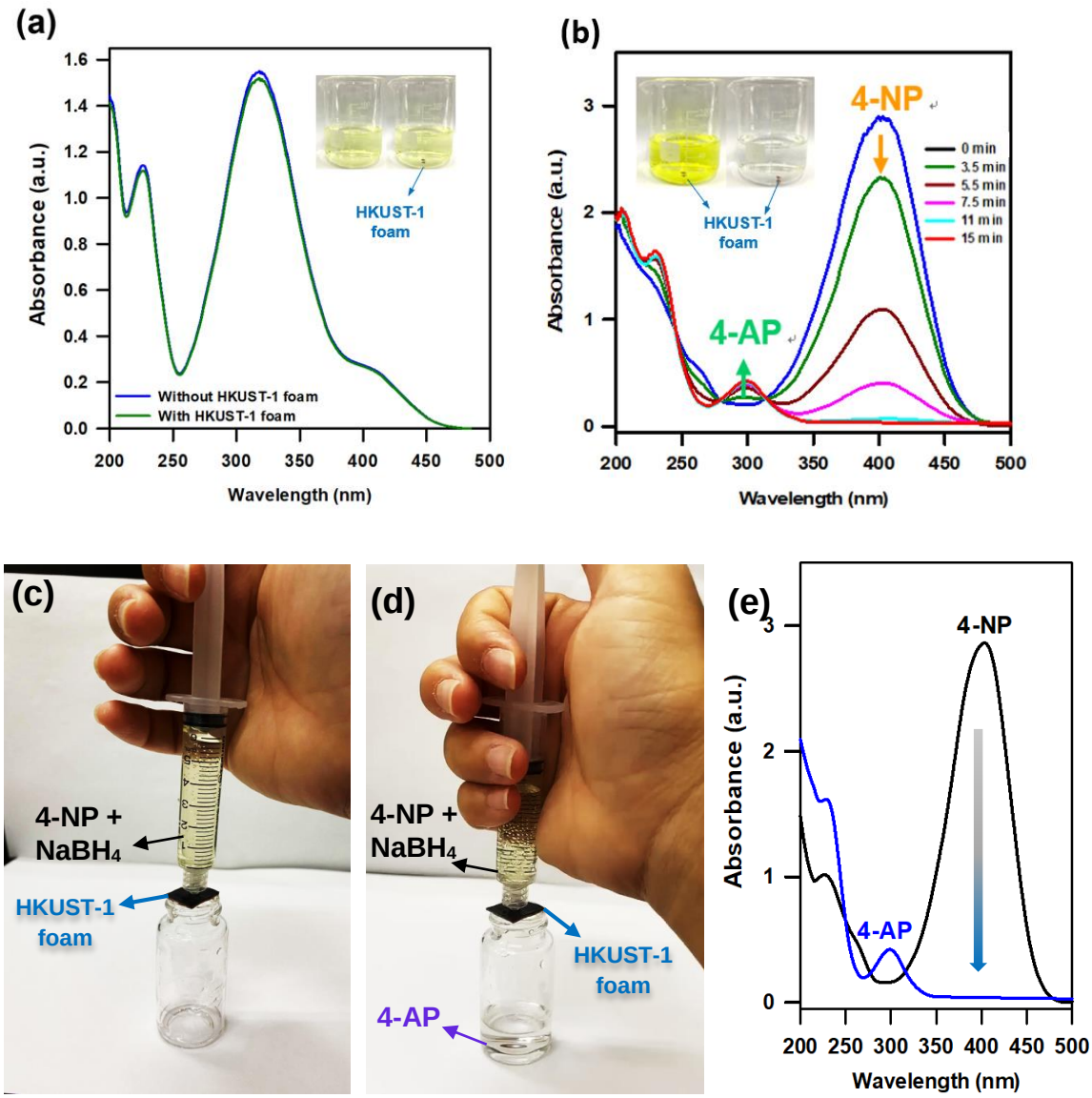

Fig. 5. (a) UV-vis absorption spectra of 4-NP solution with and without HKUST-1; (b) time-dependent (15 min) UV-vis absorption spectra during 4-NP (400 nm) reduction to 4-AP (304 nm) using HKUST-1 foam with $NaBH_4$ at 25℃(4-NP (1.8 mM), $NaBH_4$ (2.5 mM) and 3.5 mg of HKUST-1 foam); (c-d) flow-thru-type 4-NP reduction by HKUST-1 foam; and (e) UV-vis adsorption spectra of 4-NP reduction by HKUST-1 foam via the flow-thru process.

The influence of amount of HKUST-1 for 4NP reduction was also investigated as shown in Fig. S2. Firstly, 7 mg of HKUST-1 foam was evaluated for 4-NP reduction as displayed in Fig. 2(a). Nevertheless, the corresponding 4-NP reduction to 4-AP was too fast to quantify the variation as a function of time. When 3.5 mg of HKUST-1 foam was used, a full set of spectral variation of 4-NP reduction could be collected. While 4-NP reduction by a relatively low amount of HKUST-1 foam of 1.75 HKUST-1 foam can be also quantified, the reaction was much slower than that by 3.5 mg of HKUST-1. The amount of 3.5 mg was particularly selected over the course of this study.

3.3 Kinetic of 4-NP Reduction by HKUST-1 foam

As 4-NP was rapidly reduced to 4-AP by HKUST-1 foam, the reduction kinetics was further quantified using the pseudo-first rate low as follows [42-44]:

$$Ln\ (C_t/C_0) = -kt \qquad (1)$$

Where C_t is the concentration of 4-NP at a reaction time 't', C_0 is the initial concentration of 4-NP and 'k' is the first-order rate constant of 4-NP reduction over HKUST-1 foam in the presence of $NaBH_4$. The corresponding 1st-order rate constant was then calculated as 0.204 min^{-1} at 25 °C.

To further compare the catalytic activity of HKUST-1 foam with other reported catalysts, activity factors (AF) and turn over frequencies (TOF) of relevant reported catalysts are calculated using the following equations and summarized in Table 2 [45-51].

$$AF = K = k/m_{HKUST\text{-}1} \qquad (2)$$

$$TOF = n_{4\text{-}NP}/(t \times n \text{ of Cu@HKUST-1-foam}) \qquad (3)$$

where $n_{4\text{-}NP}$ is the mole of 4-NP converted, n of Cu@HKUST-1-foam is the mole of Cu within HKUST-1 foam, t is conversion time (15 min), $m_{HKUST\text{-}1}$ is amount of catalyst (g),

and *k* is the first-order rate constant of reaction. Based on gravimetric measurements, the amount of HKUST-1 on HKUST-1 foam accounted for 7 wt% of entire HKUST-1 foam. The amount of Cu within HKUST-1 foam was determined according to the molecular formula of HKUST-1 as $Cu_3(BTC)_2$ [52]. As the molecular weight of HKUST-1 is 604.87 g/mole, the amount of Cu within HKUST-1 foam could be estimated as 10.5 mol% of HKUST-1. Interestingly, in comparison with the many reported catalysts, HKUST-1 foam had certainly exhibited noticeably higher TOF and AF than many reported Cu-based and other catalysts [45-50], validating that HKUST-1 foam was a promising catalyst for 4-NP reduction.

Table 1. Comparison of rate constant(*k*), turnover frequency (TOF) and activity factor (K) of HKUST-1 foam and different reported Cu-based and other catalysts for the reduction of 4-NP.

Catalysts	$k(s^{-1})$ at room temperature	TOF (min^{-1})	AF,K($s^{-1}g^{-1}$)	Ref.
HKUST-1 foam	**0.0034**	**48.3**	**136**	**This work**
Prussian Blue (Fe)	0.0002	0.58	114	[45]
$Cu_{1.00}$–CeO_2–Pt	0.451	15.59		[46]
$Cu_{0.66}Co_{0.34}$–CeO_2–Pt	0.995	14.7		
$Cu_{0.50}Co_{0.50}$–CeO_2–Pt	0.633	8		
Cu0.34Co0.66–CeO2–Pt	0.614	7.65		
$Cu_{1.00}$–CeO_2–Pt	0.555	2.6		
CeO_2–Pt	0.285	1.55		
Cu NPs	0.0016	4.8	-	[47]
Cu hydrosol 2.01 nm	0.0037	nd	63	[48]
Cu hydrosol 5.21 nm	0.0016		28	
Cu hydrosol 9.42 nm	0.0011		19	
Cu hydrosol 17.36 nm	0.0007		12	
Cu hydrosol 26.26 nm	0.0004		6	
Porous Cu microsphere	0.0041	-	82	
Oh Cu_2O	0.0123	-	124	[49]
DHP Cu_2O	0.0056	-	5.59	
EHP Cu_2O	0.0033	-	3.28	
Cu nanoplate	0.0095	-	136	[50]
Cu 9.5 nm cubes	0.0101	-	105	[51]
Cu 18.0 nm cubes	0.0057	-	60	
Cu 21.5 nm cubes	0.0041	-	43	

To probe in the mechanism of 4-NP reduction to 4-AP by HKUST-1 foam, the chemical compositions and the elemental status of HKUST-1 foam and even the pristine Cu foam were further investigated by XPS in Fig. 6. In the case of the pristine Cu foam (Fig. 6(a)), the core-level Cu 2p spectrum displayed two major peaks at 932.4 and 952.3 eV which were attributed to Cu $2p_{3/2}$ and Cu $2p_{1/2}$, respectively [33]. On the other hand, when the pristine Cu foam was converted to HKUST-1 foam (Fig. 6(b)), the Cu $2p_{3/2}$ and Cu $2p_{1/2}$ peaks of HKUST-1 foam shifted to the higher binding energies of 933.5 and 953.4 eV, respectively, revealing the occurrence of Cu^{2+} [16]. Besides, additional four peaks can be also detected at 939.5, 943.2, 959.3, and 962.8 eV which were derived from the Cu^{2+} satellite peaks [33, 53]. However, once HKUST-1 foam participated in 4-NP reduction, the used HKUST-1 (Fig. 6(c)) not only exhibited Cu^{2+} at 932.4 and 952.2 eV but also showed Cu^{+} species at 934.4 and 954.3 eV [54].

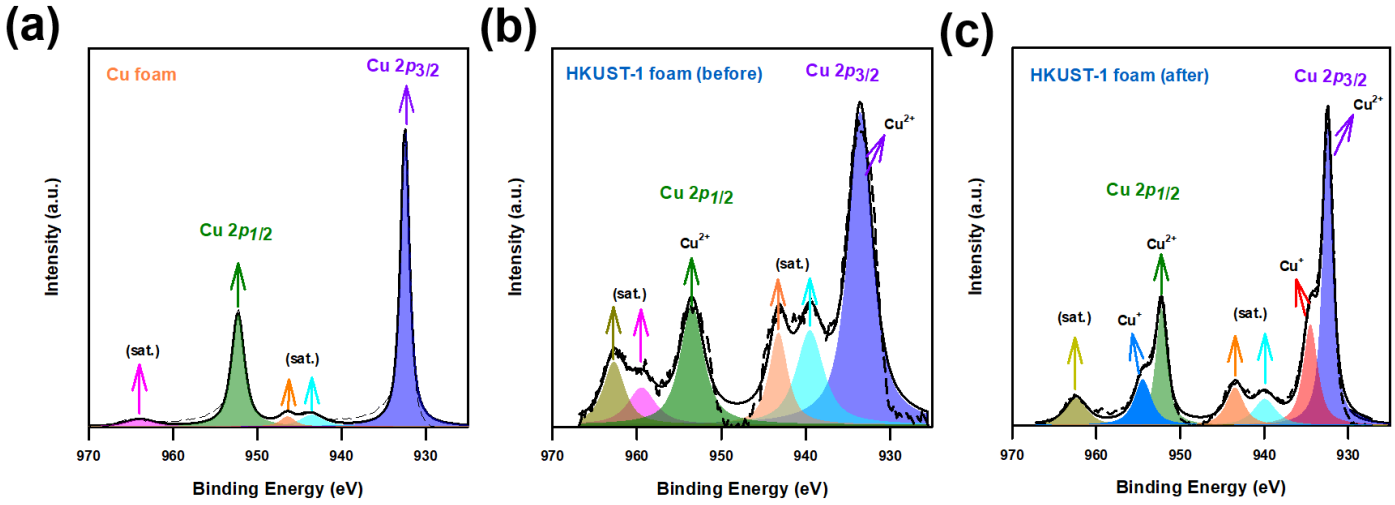

Fig. 6. XPS spectra of Cu foam and HKUST-1 foam before and after 4-NP reduction: (a) Cu 2p of Cu foam, (b) Cu 2p (before) of HKUST-1 foam, (c) Cu 2p (after) of HKUST-1 foam.

Based on the XPS results, the possible mechanism of reduction of 4-NP to 4-AP by HKUST-1 foam would be depicted in Fig. 7. Firstly, HKUST-1 foam reacted with

$NaBH_4$ to release H_2 gas [55, 56] which would further reduce Cu^{2+} to Cu^{+}. After 4-NP was adsorbed to HKUST-1 foam, and its nitro-group would receive electrons from Cu^{+} together with H^{+} from the solution to be hydrogenated, forming 4-AP [57, 58], while Cu^{+} was transferred back to Cu^{2+}. Finally, 4-AP was desorbed from the surface of HKUST-1 foam and went back to the solution.

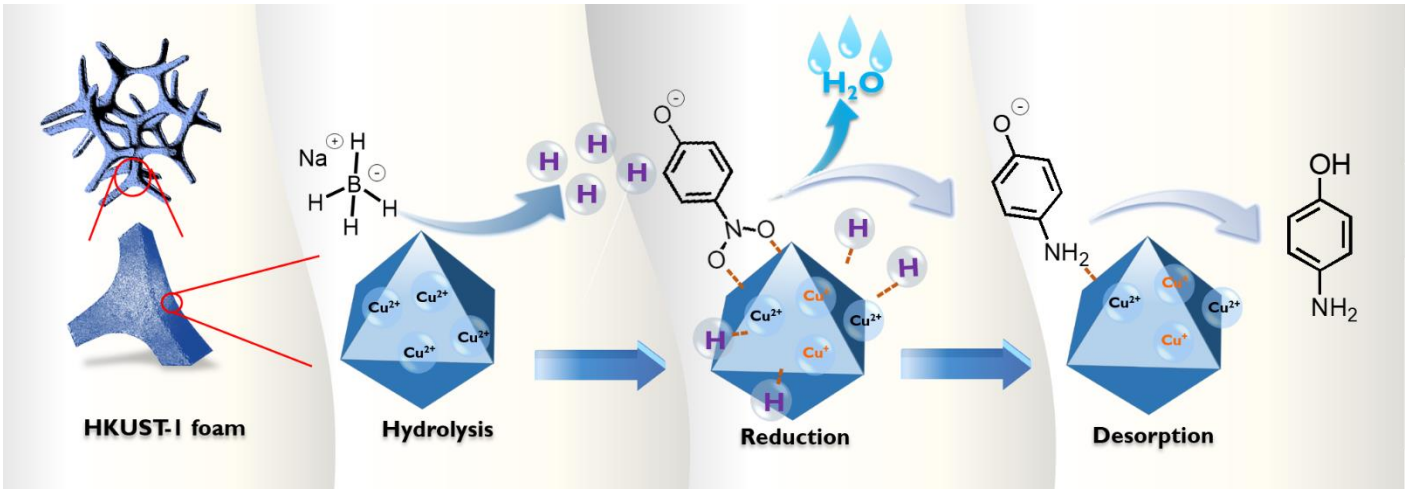

Fig. 7. Schematic illustration of plausible mechanism of 4-NP reduction by HKUST-1 foam in the presence of $NaBH_4$.

3.4 Activation energy (E_a) of 4-NP reduction by HKUST-1 foam

As activation energy (E_a) represents an important index for evaluating catalytic activities of catalysts for 4-NP reduction, the corresponding *Ea* by HKUST-1 foam was then obtained from kinetics of 4-NP reduction at different temperatures as exhibited in Table S1. Fig. S3 showed the Arrhenius plots (*ln k* vs *1/T*), and the corresponding E_a (the activation energy) was obtained as 43.3 kJ/mol. Compared to other catalysts (Table 3), the Ea value by HKUST-1 foam was noticeably lower than many reported catalysts, especially noble catalysts [59-63]. This indicates the promising advantage of HKUST-

1 foam for reduction of 4-NP possibly because Cu has been a widely-recognized effective metal for 4-NP reduction [45, 51, 64], and HKUST-1 is the most classical and well-known Cu-based MOFs [65]. As HKUST-1 exhibits a relatively high surface area and a relatively large pore volume in comparison to reported Cu catalysts, more active site of Cu^{2+} from HKUST-1 would be available and exposing to reactants (e.g., 4-NP and $NaBH_4$), facilitating 4-NP reduction.

Table 2. Comparison of activation energies (E_a) of HKUST-1 foam and different reported catalysts for the reduction of 4-NP.

Catalyst	E_a (kJ/mol)	Ref.
HKUST-1 foam	**43.3**	This work
NiY	105	[59]
PtY	136	
CoY	60	
PtNiY	119	
PtCoY	55	
Pt NPs	40	[60]
Magnetic Au-NP	51	[61]
PS-PEGMA-Ag	62	[62]
Cu^{2+}	74	[63]
Ag^{+}	173.1	
$AuCl_4^{-}$	32.6	
Co^{2+}	34.7	
Ni^{2+}	216.4	

3.5 Reusability of HKUST-1 foam for 4-NP reduction

As HKUST-1 foam was proposed to be an easy-to-use and practical catalyst for 4-NP, HKUST-1 should be reusable for long-term 4-NP reduction. Thus, the reusability of HKUST-1 foam was investigated by reusing HKUST-1 foam for multi-cycle 4-NP reduction without any regeneration. Fig. 8 shows results of 4-NP reduction of 5 cycle by the used HKUST-1 foam, which still exhibited very comparable catalytic activities for reducing 4-NP to 4-AP without significant loss of reactivities. Even though the reduction kinetics seemed slightly decreased (0.204 to 0.202 min^{-1}), this phenomenon

might be attributed to the fact that by-products from $NaBH_4$ would remain in the solution or adsorb to HKUST-1 foam, interfering with contacts between 4-NP, HKUST-1 and BH_4^- ion, and altered the kinetics.

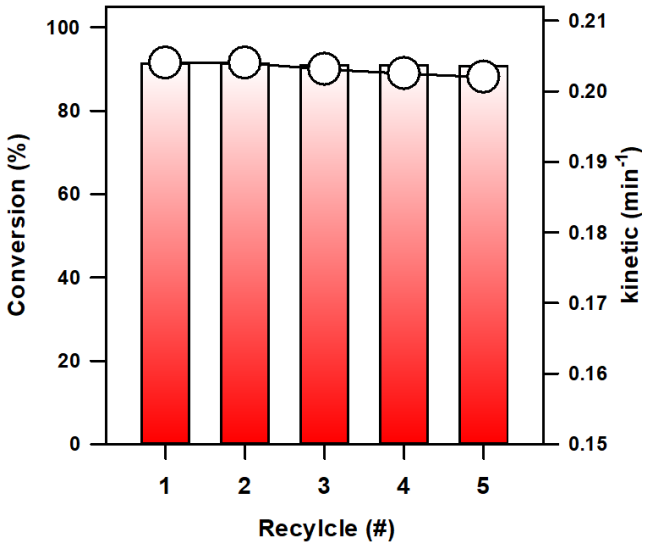

Fig. 8. Reusability of HKUST-1 foam for multiple-cycle 4-NP reduction

3.6 Catalytic performance of HKUST-1 for Methylene Blue

In addition to 4-NP reduction, the catalytic hydrogenation would be also employed for decolorizing dye-containing wastewater [66-68]. Specifically, Methylene blue (MB) represents an extensively-used dye and it could be decolorized by hydrogenate its nitrogen group of phenothiazine in MB [66-68]. Firstly, Fig. S4 shows a MB aqueous solution (curve a) and a MB solution in the presence of HKUST-1 foam after 300 min (curve b), indicating that adsorption of MB adsorbed to HKUST-1 was negligible. Subsequently, after $NaBH_4$ was added to MB solution in the presence of HKUST-1 foam (Fig. 9(a)), the blue color of MB rapidly decreased within 3 min and no by-product was present based on Fig. 9 (b). The corresponding pseudo-first order rate constant was 1.67 min^{-1}, which was significantly higher than many reported values of MB hydrogenation [69-74] (Table 3), indicating its superior catalytic activities for aqueous

hydrogenation of MB.

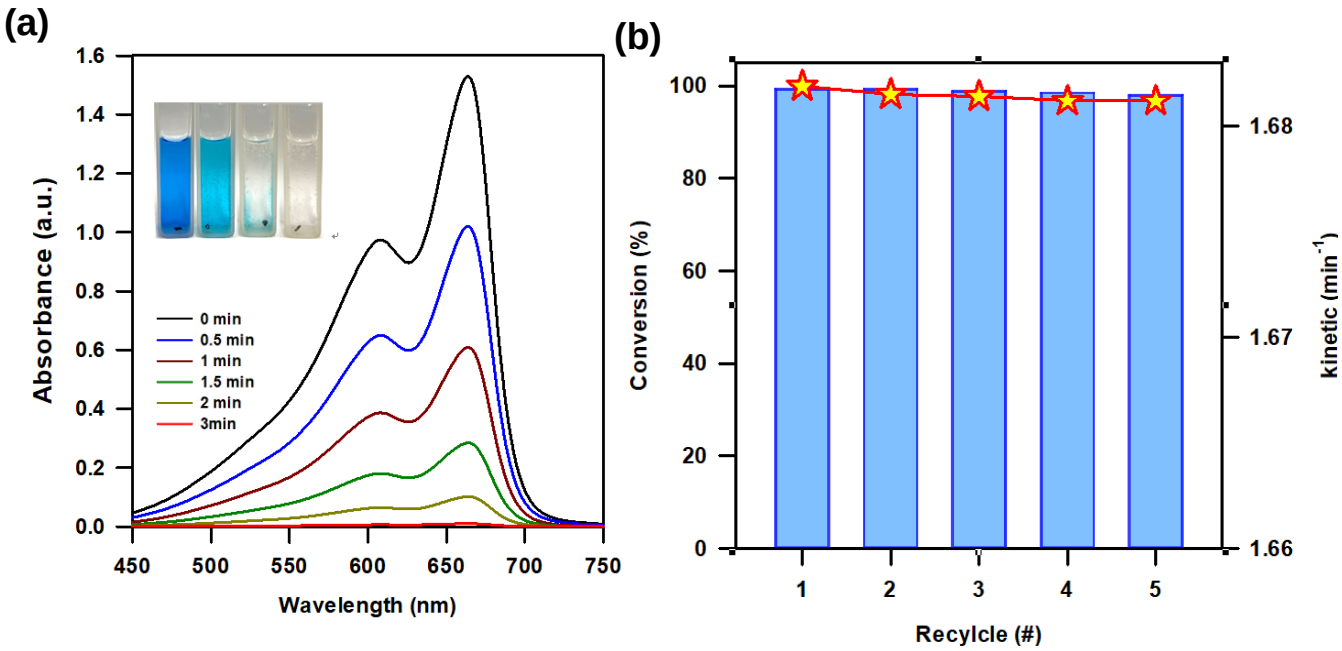

Fig. 9. (a) Time-dependents UV-vis absorption spectra of MB during reduction using HKUST-1 foam in the presence of $NaBH_4$ and (b) reusability of HKUST-1 foam for multiple-cycle reduction of MB.

Additionally, we also examined reusability of HKUST-1 foam in MB reduction as exhibited in Fig. 9(b). A fresh MB aqueous solution was prepared after completing every cycle. HKUST-1 foam exhibited almost identical catalytic performance of every cycle without regeneration. According to these results, HKUST-1 foam had high effective catalytic performance not only for 4-NP but also for MB. This result demonstrated that HKUST-1 foam is a stable and favorable catalyst for catalytic reduction.

Table 3. Comparison of rate constant (k) of HKUST-1 foam and different reported catalysts for the reduction of MB.

Catalyst	*k* at room temperature (min^{-1})	Ref.
HKUST-1 foam	**1.6658**	**This work**
Pd/Si	1.436	[69]
pNAC7	0.7959	[70]
C-Pt NPs	0.03	[71]
MgAl-LDH@Au	0.84	[72]
MgAlCe-LDH@Au	1.8	
MgAlCe-LDH	0.3	
AgNPs	0.199	[73]
cotton@Ag NPs	0.478	[74]

4. Conclusion

In conclusion, a 3D-structured hierarchical composite of HKUST-1 foam was developed via one-step electrochemical growth of HKUST-1 on Cu-foam. The Cu-foam served not only as the support for HKUST-1 but also a source of Cu for synthesizing HKUST-1. Thus, HKUST-1 formed on the surface of foam could still exhibit polyhedral shapes and maintained its porous features. More importantly, the resulting HKUST-1 foam can further act as an easy-to-use heterogeneous catalyst for reduction of 4-NP to 4-AP. The corresponding *Ea* of 4-NP reduction was also significantly lower than *Ea* values of reported catalysts, including noble metal catalysts, whereas the corresponding TOF was higher than many other catalysts, revealing its promising advantage. In addition, HKUST-1 foam could be reused over multi-cycles and retained its crystalline structure and catalytic activity for 4-NP reduction. Through XPS analysis, the mechanism of 4-NP reduction catalyzed by HKUST-1 foam could then be attributed to the reduction of Cu site of HKUST-1 by $NaBH_4$ and then electrons transferred from Cu^+ together with H^+ to hydrogenate 4-NP to 4-AP. These features validate that

HKUST-1 foam is certainly a practical, convenient, effective and reusable catalyst for reduction of 4-NP and MB.

References:

1. Ji, Y.F., et al., *Rethinking sulfate radical-based oxidation of nitrophenols: Formation of toxic polynitrophenols, nitrated biphenyls and diphenyl ethers.* Journal of Hazardous Materials, 2019. **361**: p. 152-161.
2. Narayanan, K.B. and N. Sakthivel, *Synthesis and characterization of nano-gold composite using Cylindrocladium floridanum and its heterogeneous catalysis in the degradation of 4-nitrophenol.* Journal of Hazardous Materials, 2011. **189**(1-2): p. 519-525.
3. EPA, A.a., *Toxicology Profile for Nitrophenols: 2-Nitrophenol, 4-Nitrophenol*, A.f.T.S.a.D. Registry, Editor. 1992.
4. Subashchandrabose, S.R., et al., *Rhodococcus wratislaviensis strain 9: An efficient p-nitrophenol degrader with a great potential for bioremediation.* Journal of Hazardous Materials, 2018. **347**: p. 176-183.
5. Guzman, M., et al., *Synthesis of cerium oxide (IV) hollow nanospheres with tunable structure and their performance in the 4-nitrophenol adsorption.* Microporous and Mesoporous Materials, 2019. **278**: p. 241-250.
6. Garcia, D.T., et al., *Photocatalytic ozonation under visible light for the remediation of water effluents and its integration with an electro-membrane bioreactor.* Chemosphere, 2018. **209**: p. 534-541.
7. Wi-Afedzi, T., et al., *A comparative study of hexacyanoferrate-based Prussian blue analogue nanocrystals for catalytic reduction of 4-nitrophenol to 4-aminophenol.* Separation and Purification Technology, 2019. **218**: p. 138-145.
8. Deka, P., R.C. Deka, and P. Bharali, *In situ generated copper nanoparticle catalyzed reduction of 4-nitrophenol.* New Journal of Chemistry, 2014. **38**(4): p. 1789-1793.
9. Kohantorabi, M. and M.R. Gholami, *Kinetic Analysis of the Reduction of 4-Nitrophenol Catalyzed by CeO2 Nanorods-Supported CuNi Nanoparticles.* Industrial & Engineering Chemistry Research, 2017. **56**(5): p. 1159-1167.
10. Tafesh, A.M. and J. Weiguny, *A review of the selective catalytic reduction of aromatic nitro compounds into aromatic amines, isocyanates, carbamates, and ureas using CO.* Chemical Reviews, 1996. **96**(6): p. 2035-2052.
11. Andrew Lin, K.-Y., H.-A. Chang, and C.-J. Hsu, *Iron-based metal organic framework, MIL-88A, as a heterogeneous persulfate catalyst for decolorization of Rhodamine B in water.* RSC Advances, 2015. **5**(41): p. 32520-32530.

12. Lin, K.-Y.A., B.-J. Chen, and C.-K. Chen, *Evaluating Prussian blue analogues MII3[MIII(CN)6]2 (MII = Co, Cu, Fe, Mn, Ni; MIII = Co, Fe) as activators for peroxymonosulfate in water.* RSC Advances, 2016. **6**(95): p. 92923-92933.
13. Yun, W.-C., M.-T. Yang, and K.-Y.A. Lin, *Water-born zirconium-based metal organic frameworks as green and effective catalysts for catalytic transfer hydrogenation of levulinic acid to γ-valerolactone: Critical roles of modulators.* Journal of Colloid and Interface Science, 2019. **543**: p. 52-63.
14. Lin, K.-Y.A. and H.-A. Chang, *Zeolitic Imidazole Framework-67 (ZIF-67) as a heterogeneous catalyst to activate peroxymonosulfate for degradation of Rhodamine B in water.* Journal of the Taiwan Institute of Chemical Engineers, 2015. **53**: p. 40-45.
15. Wi-Afedzi, T., et al., *A comparative study of hexacyanoferrate-based Prussian blue analogue nanocrystals for catalytic reduction of 4-nitrophenol to 4-aminophenol.* Separation and Purification Technology, 2019. **218**: p. 138-145.
16. Wi-Afedzi, T., et al., *Copper hexacyanoferrate nanocrystal as a highly efficient non-noble metal catalyst for reduction of 4-nitrophenol in water.* Science of The Total Environment, 2020. **703**: p. 134781.
17. Huang, D., et al., *Assembling of a novel 3D Ag(I)-MOFs with mixed ligands tactics: Syntheses, crystal structure and catalytic degradation of nitrophenol.* Chinese Chemical Letters, 2018. **29**(6): p. 845-848.
18. Andrew Lin, K.-Y. and Y.-T. Hsieh, *Copper-based metal organic framework (MOF), HKUST-1, as an efficient adsorbent to remove p-nitrophenol from water.* Journal of the Taiwan Institute of Chemical Engineers, 2015. **50**: p. 223-228.
19. Liu, J., H. Yu, and L. Wang, *Effective reduction of 4-nitrophenol with Au NPs loaded ultrathin two dimensional metal-organic framework nanosheets.* Applied Catalysis A: General, 2020. **599**: p. 117605.
20. Singh, K., et al., *In situ green synthesis of Au/Ag nanostructures on a metal-organic framework surface for photocatalytic reduction of p-nitrophenol.* Journal of Industrial and Engineering Chemistry, 2020. **81**: p. 196-205.
21. Sadeghzadeh, S.M., R. Zhiani, and S. Emrani, *The reduction of 4-nitrophenol and 2-nitroaniline by the incorporation of Ni@Pd MNPs into modified UiO-66-NH2 metal–organic frameworks (MOFs) with tetrathia-azacyclopentadecane.* New Journal of Chemistry, 2018. **42**(2): p. 988-994.
22. Andrew Lin, K.-Y. and H.-A. Chang, *A zeolitic imidazole framework (ZIF)–sponge composite prepared via a surfactant-assisted dip-coating method.* Journal of Materials Chemistry A, 2015. **3**(40): p. 20060-20064.
23. Chen, Y.-J., et al., *Metal–organic framework-based foams for efficient*

microplastics removal. Journal of Materials Chemistry A, 2020. **8**(29): p. 14644-14652.

24. Pinto, M.L., S. Dias, and J. Pires, *Composite MOF Foams: The Example of UiO-66/Polyurethane.* ACS Applied Materials & Interfaces, 2013. **5**(7): p. 2360-2363.
25. Senthil Raja, D., H.-W. Lin, and S.-Y. Lu, *Synergistically well-mixed MOFs grown on nickel foam as highly efficient durable bifunctional electrocatalysts for overall water splitting at high current densities.* Nano Energy, 2019. **57**: p. 1-13.
26. Huang, N., et al., *Flexible and Hierarchical Metal–Organic Framework Composites for High-Performance Catalysis.* Angewandte Chemie International Edition, 2018. **57**(29): p. 8916-8920.
27. Deng, Y.H., et al., *Multifunctional Mesoporous Composite Microspheres with Well-Designed Nanostructure: A Highly Integrated Catalyst System.* Journal of the American Chemical Society, 2010. **132**(24): p. 8466-8473.
28. Elfiad, A., et al., *Natural alpha-Fe2O3 as an efficient catalyst for the p-nitrophenol reduction.* Materials Science and Engineering B-Advanced Functional Solid-State Materials, 2018. **229**: p. 126-134.
29. Wee, L.H., et al., *Fine tuning of the metal–organic framework Cu3(BTC)2 HKUST-1 crystal size in the 100 nm to 5 micron range.* Journal of Materials Chemistry, 2012. **22**(27).
30. Zhou, L., et al., *Effect of Lithium Doping on the Structures and CO2 Adsorption Properties of Metal-Organic Frameworks HKUST-1.* ChemistrySelect, 2018. **3**(45): p. 12865-12870.
31. Wang, F., et al., *The controlled regulation of morphology and size of HKUST-1 by "coordination modulation method".* Microporous and Mesoporous Materials, 2013. **173**: p. 181-188.
32. Zhou, J., et al., *Superhydrophobic Cu-based materials with excellent durability, stability, and regenerability grounded of self-similarity.* Applied Physics A, 2019. **125**(6).
33. Wang, Z., et al., *Yucca fern shaped CuO nanowires on Cu foam for remitting capacity fading of Li-ion battery anodes.* Sci Rep, 2018. **8**(1): p. 6530.
34. Lin, J.-Y., et al., *Selective aerobic oxidation of 5-hydroxymethylfurfural to 2,5-diformylfuran catalyzed by Cu-based metal organic frameworks with 2,2,6,6-tetramethylpiperidin-oxyl.* Journal of the Taiwan Institute of Chemical Engineers, 2019. **102**: p. 242-249.
35. Tan, P., et al., *Fabrication of magnetically responsive HKUST-1/Fe3O4 composites by dry gel conversion for deep desulfurization and*

denitrogenation. J Hazard Mater, 2017. **321**: p. 344-352.

36. Yang, A., P. Li, and J. Zhong, *Facile preparation of low-cost HKUST-1 with lattice vacancies and high-efficiency adsorption for uranium.* RSC Advances, 2019. **9**(18): p. 10320-10325.
37. Chen, M., et al., *Two-Step Elution Recovery of Cyanide Platinum Using Functional Metal Organic Resin.* Molecules, 2019. **24**(15).
38. Maleki, A., et al., *Adsorption of hexavalent chromium by metal organic frameworks from aqueous solution.* Journal of Industrial and Engineering Chemistry, 2015. **28**: p. 211-216.
39. Peng, L., et al., *Hollow metal-organic framework polyhedra synthesized by a CO2-ionic liquid interfacial templating route.* J Colloid Interface Sci, 2014. **416**: p. 198-204.
40. Foo, K.Y. and B.H. Hameed, *Insights into the modeling of adsorption isotherm systems.* Chemical Engineering Journal, 2010. **156**(1): p. 2-10.
41. Xu, Y., et al., *Remarkably catalytic activity in reduction of 4-nitrophenol and methylene blue by Fe3O4@COF supported noble metal nanoparticles.* Applied Catalysis B: Environmental, 2020. **260**.
42. Chen, R., et al., *One-pot green synthesis of Prussian blue nanocubes decorated reduced graphene oxide using mushroom extract for efficient 4-nitrophenol reduction.* Analytica Chimica Acta, 2015. **853**: p. 579-587.
43. Lin, F.-h. and R.-a. Doong, *Bifunctional Au–Fe3O4 Heterostructures for Magnetically Recyclable Catalysis of Nitrophenol Reduction.* The Journal of Physical Chemistry C, 2011. **115**(14): p. 6591-6598.
44. Zhang, P., et al., *Facile fabrication of faceted copper nanocrystals with high catalytic activity for p-nitrophenol reduction.* Journal of Materials Chemistry A, 2013. **1**(5): p. 1632-1638.
45. Wi-Afedzi, T., et al., *Copper hexacyanoferrate nanocrystal as a highly efficient non-noble metal catalyst for reduction of 4-nitrophenol in water.* Sci Total Environ, 2020. **703**: p. 134781.
46. Wang, F., et al., *Decoration of Pt on Cu/Co double-doped CeO2 nanospheres and their greatly enhanced catalytic activity.* Chem Sci, 2016. **7**(3): p. 1867-1873.
47. Deka, P., R.C. Deka, and P. Bharali, *In situ generated copper nanoparticle catalyzed reduction of 4-nitrophenol.* New Journal of Chemistry, 2014. **38**(4).
48. Zhang, Y., et al., *Highly stable and re-dispersible nano Cu hydrosols with sensitively size-dependent catalytic and antibacterial activities.* Nanoscale, 2015. **7**(32): p. 13775-83.
49. Aditya, T., et al., *Remarkable Facet Selective Reduction of 4-Nitrophenol by*

Morphologically Tailored (111) Faceted Cu2O Nanocatalyst. ACS Omega, 2017. **2**(5): p. 1968-1984.

50. Sun, Y., et al., *Synthesis of copper submicro/nanoplates with high stability and their recyclable superior catalytic activity towards 4-nitrophenol reduction.* Journal of Materials Chemistry A, 2013. **1**(39).
51. Zhang, P., et al., *Facile fabrication of faceted copper nanocrystals with high catalytic activity for p-nitrophenol reduction.* J. Mater. Chem. A, 2013. **1**(5): p. 1632-1638.
52. Lin, K.-S., et al., *Synthesis and characterization of porous HKUST-1 metal organic frameworks for hydrogen storage.* International Journal of Hydrogen Energy, 2012. **37**(18): p. 13865-13871.
53. Rivera-Torrente, M., et al., *Micro-spectroscopy of HKUST-1 metal-organic framework crystals loaded with tetracyanoquinodimethane: effects of water on host-guest chemistry and electrical conductivity.* Phys Chem Chem Phys, 2019. **21**(46): p. 25678-25689.
54. Thomas Waechtler, S.O., Nina Roth, Alexander Jakob, Heinrich Lang, Ramona Ecke, Stefan E. Schulz, Thomas Gessner, Anastasia Moskvinova, Steffen Schulze, *Copper Oxide Films Grown by Atomic Layer Deposition from Bis(tri-n-butylphosphane)copper(I)acetylacetonate on Ta, TaN, Ru, and SiO2.* Journal of The Electrochemical Society, 2009. **156**(6): p. H453-H459.
55. Demirci, S. and N. Sahiner, *Superior reusability of metal catalysts prepared within poly(ethylene imine) microgels for H2 production from NaBH4 hydrolysis.* Fuel Processing Technology, 2014. **127**: p. 88-96.
56. Balbay, A. and C. Saka, *Effect of phosphoric acid addition on the hydrogen production from hydrolysis of NaBH4 with Cu based catalyst.* Energy Sources, Part A: Recovery, Utilization, and Environmental Effects, 2018. **40**(7): p. 794-804.
57. Shi, D., et al., *Ultra-small and recyclable zero-valent iron nanoclusters for rapid and highly efficient catalytic reduction of p-nitrophenol in water.* Nanoscale, 2019. **11**(3): p. 1000-1010.
58. Bae, S., et al., *Effect of NaBH4 on properties of nanoscale zero-valent iron and its catalytic activity for reduction of p-nitrophenol.* Applied Catalysis B: Environmental, 2016. **182**: p. 541-549.
59. El-Bahy, Z.M., *Preparation and characterization of Pt-promoted NiY and CoY catalysts employed for 4-nitrophenol reduction.* Applied Catalysis A: General, 2013. **468**: p. 175-183.
60. Stefanie Wunder, F.P., Yan Lu, Yu Mei, and Matthias Ballauff, *Kinetic Analysis of Catalytic Reduction of 4-Nitrophenol by Metallic Nanoparticles Immobilized*

in Spherical Polyelectrolyte Brushes. J. Phys. Chem. C, 2010. **114**(19): p. 8814-8820.

61. Chang, Y.C. and D.H. Chen, *Catalytic reduction of 4-nitrophenol by magnetically recoverable Au nanocatalyst.* J Hazard Mater, 2009. **165**(1-3): p. 664-9.
62. Lu, Y., et al., *'Nano-tree'—type spherical polymer brush particles as templates for metallic nanoparticles.* Polymer, 2006. **47**(14): p. 4985-4995.
63. Wu, X.-Q., et al., *In situ formed metal nanoparticle systems for catalytic reduction of nitroaromatic compounds.* RSC Adv., 2014. **4**(90): p. 49287-49294.
64. Jiang, J., et al., *Hierarchical Cu nanoparticle-aggregated cages with high catalytic activity for reduction of 4-nitrophenol and carbon dioxide.* Materials Research Bulletin, 2018. **100**: p. 184-190.
65. Chen, Y., et al., *High efficiency synthesis of HKUST-1 under mild conditions with high BET surface area and CO2 uptake capacity.* Progress in Natural Science: Materials International, 2018. **28**(5): p. 584-589.
66. Rajegaonkar, P.S., et al., *Catalytic reduction of p-nitrophenol and methylene blue by microbiologically synthesized silver nanoparticles.* Materials Science and Engineering: C, 2018. **93**: p. 623-629.
67. Xu, Y., et al., *Remarkably catalytic activity in reduction of 4-nitrophenol and methylene blue by Fe3O4@COF supported noble metal nanoparticles.* Applied Catalysis B: Environmental, 2020. **260**: p. 118142.
68. Sahiner, N., S. Sagbas, and N. Aktas, *Very fast catalytic reduction of 4-nitrophenol, methylene blue and eosin Y in natural waters using green chemistry: p(tannic acid)–Cu ionic liquid composites.* RSC Advances, 2015. **5**(24): p. 18183-18195.
69. Hui Hu, M.S., Wu Zhang, Lei Lu, Hong Wang, and Sheng Wang, *Synthesis of Layer-Deposited Silicon Nanowires, Modification with Pd Nanoparticles, and Their Excellent Catalytic Activity and Stability in the Reduction of Methylene Blue.* The Journal of Physical Chemistry C, 2007. **111**: p. 3467-6470.
70. Shah, L.A., et al., *Ag-loaded thermo-sensitive composite microgels for enhanced catalytic reduction of methylene blue.* Nanotechnology for Environmental Engineering, 2017. **2**(1).
71. You, J.G., et al., *Boosting catalytic activity of metal nanoparticles for 4-nitrophenol reduction: Modification of metal naoparticles with poly(diallyldimethylammonium chloride).* J Hazard Mater, 2017. **324**(Pt B): p. 420-427.
72. Iqbal, K., et al., *A new Ce-doped MgAl-LDH@Au nanocatalyst for highly*

efficient reductive degradation of organic contaminants. Journal of Materials Chemistry A, 2017. **5**(14): p. 6716-6724.

73. Li, Z., et al., *Preparation of stable AgNPs@PAN/GO-SH nanocompsite by electrospinning for effective degradation of 4-nitrophenol, methylene blue and Rhodamine B.* Materials Letters, 2020. **265**.
74. Qi, L., et al., *Highly efficient flow-through catalytic reduction of methylene blue using silver nanoparticles functionalized cotton.* Chemical Engineering Journal, 2020. **388**.

Declaration of interests

☒ The authors declare that they have no known competing financial interests or personal relationships that could have appeared to influence the work reported in this paper.

☐The authors declare the following financial interests/personal relationships which may be considered as potential competing interests: